Capillary Morphogenesis gene 2 mediates multiple pathways of growth factor-induced angiogenesis by regulating endothelial cell chemotaxis

Lorna Cryan [b,‡], Tsz-Ming Tsang [a,‡], Jessica Stiles [b], Lauren Bazinet [b], Sai Lun Lee[a], Samuel Garrard[a], Cody Roberts[a], Jessie Payne[a], P. Christine Ackroyd[a], Kenneth A. Christensen[a], Michael S. Rogers[b]

[a]Department of Chemistry and Biochemistry, Brigham Young University, Provo, Utah, United States of America 84602. T. Tsang, jeremytmtsang@outlook.com; S.L. Lee, leesailun91@gmail.com; S. Garrard, sam.garrard@byu.edu; C. Roberts, cdejames3@gmail.com; P.C. Ackroyd, ackroyd@byu.edu

[b]Department of Surgery, Vascular Biology Program, Children's Hospital Boston, Harvard Medical School, Boston, Massachusetts, United States of America 02115. Email: M.S. Rogers, Michael.rogers@childrens.harvard.edu

Abstract

Pathological angiogenesis contributes to diseases as varied as cancer and corneal neovascularization. The vascular endothelial growth factor (VEGF) - VEGF receptor 2 (KDR/VEGFR2) axis has been the major target for treating pathological angiogenesis. However, VEGF-targeted therapies exhibit modest efficacy over time indicating that new therapeutic strategies are needed. Therefore, identifying new targets that mediate angiogenesis is of great importance. Here, we report that one of the anthrax toxin receptors, capillary morphogenesis gene 2 (ANTXR2/CMG2), plays an important role in mediating angiogenesis. Inhibiting physiological ligand binding to CMG2 results in significant reduction of corneal neovascularization, endothelial tube formation and cell migration. We also report the novel finding that CMG2 mediates angiogenesis by regulating the direction of endothelial chemotactic migration without affecting overall cell motility.

Introduction

Pathological angiogenesis is closely related to many diseases including cancers and various ocular diseases that lead to blindness. Most of the current treatment strategies are targeting the VEGF - VEGFR2 axis. However, such therapies only provide modest efficacy overtime and accompany with unpleasant side effects. Thus, identify new targets are needed and is critical for alternative therapeutic strategies development. It was previously demonstrated that one of the anthrax toxin receptors, CMG2, has a role in mediating angiogenesis[1, 2]. Our previous work demonstrated that inhibition of CMG2 potently reduces angiogenesis in the cornea[1] and inhibit endothelial cell migration[3, 4]. Thus, we are interested to investigate the role(s) of CMG2 in mediating angiogenesis.

While the knowledge of CMG2's role in angiogenesis remain limited, its function as one of anthrax toxin receptors, is very well established. CMG2 and its homolog, tumor endothelial

39 marker 8 (ANTXR1 / TEM8), were consider the primary sites of anthrax toxins entry. Both
40 CMG2 and TEM8 share 40% amino acid homology including sharing homology in an
41 intracellular domain of unknown function that is shared with no other protein in the mammalian
42 genome[5]. Within their von Willebrand Factor A (VWA) ligand binding domains, CMG2-TEM8
43 homology rises to 60%[6]. During anthrax intoxication, the 83kDa protective antigen (PA), one of
44 the three subunits from *Bacillus anthracis*, binds to the VWA ligand binding domain of the
45 receptor. It is then cleaved by a furin-like protease that cut and releases a 20kDa fragment,
46 leaving a 63kDa PA at the receptor surface. The cleaved PA oligormerize to form and PA-
47 receptor heptamer, which acts as a binding platform for the other two toxin subunits, lethal
48 factor (LF) and edema factor (EF), and traffic the toxins into the cell via endocytosis[7].

49 The endogenous functions of the anthrax toxin receptors are still poorly understood,
50 although, it was suggest that these receptors interacts with extra-cellular matrix (ECM) proteins[2,
51 8]. Studies observed that mutations on CMG2 or TEM8 would lead to build up of hyaline
52 materials that result in implication of skeletal growth and alternation of vascular patterns. Lost of
53 function mutations in TEM8 would cause GAPO syndrome, a disease characterized by vascular
54 anomalies, skeletal defects, growth retardation and progressive fibrosis of various organs[9, 10].
55 Mutations in CMG2 in humans leads to Hyaline Fibromatosis Syndrome (HFS), a rare but
56 serious autosomal recessive disorder, characterized by accumulation of hyaline material in
57 connective tissue in the skin and other organs and by the presence of non-cancerous nodules[11-
58 13] containing excess collagen I, collagen VI, and glycosaminoglycans. To explain the
59 symptoms, it has been hypothesized that patients with a CMG2 mutation have a defect in either
60 the synthesis or degradation of ECM[12, 14], presumably related to CMG2 dysfunction.

61 In addition to ECM binding, it is suggested that these receptors have angiogenic related
62 activity[1, 15]. Our previous work demonstrated that a furin-cleavage-site mutant of protective
63 antigen (PA^{SSSR}) inhibits basic fibroblast growth factor (bFGF) induced corneal

64 neovascularization, VEGF-induced corneal neovascularization, and tumor growth[1,16]. Because
65 PA^{SSSR} is known to bind both anthrax toxin receptors (CMG2 and TEM8) as well as integrin β1[17,
66 18], it has remained unclear which of these receptors was responsible for mediating the observed
67 anti-angiogenic effect of PA^{SSSR} *in vivo*. While CMG2 has a much tighter affinity for PA than the
68 other two receptors[18-20], it is considered to be the major receptor for PA. Thus, we hypothesized
69 that CMG2 is the relevant receptor that are responsible to PA's anti-angiogenic affect.
70 Additionally, our previous data showed that CMG2 inhibition reduces angiogenesis in both in-
71 vivo and ex-vivo assays, however, the biology behind such observations remain unclear.
72 Therefore, the focuses of this paper are to understand the anti-angiogenic relationship between
73 CMG2 and PA^{SSSR}, and further investigate the role(s) of CMG2 in mediating angiogenesis in
74 endothelial cells.

75 **Result and Discussion**

76 As mentioned previously, PA^{SSSR} interacts both anthrax toxin receptors and integrin β1.
77 While CMG2 and tumor endothelial marker 8 (TEM8) bind PA^{SSSR} much more tightly than does
78 integrin β1 (Kd for CMG2, 200pM; TEM8, 100nM[18, 21]; integrin β1, 1μM), suggesting that CMG2
79 and TEM8 are more likely to mediate the antiangiogenic effects of PA^{SSSR}. We performed a
80 series of experiments to compare the relative contributions of CMG2 and TEM8 to corneal
81 neovascularization in mice, and to determine whether blockade of either of these receptors was
82 sufficient to explain the observed effect. First, we used either a CMG2 or TEM8 extracellular
83 domain fused to an antibody Fc-domain to disrupt the ligand-receptor interaction by competing
84 for endogenous ligand binding. In the corneal micropocket assay, administration of CMG2-Fc
85 significantly inhibited bFGF-induced vessel growth when compared to the untreated control, but
86 the TEM8-Fc fusion did not (Fig. 1A). We confirmed this observation by administering antibodies
87 specific to either the CMG2 or TEM8 extracellular domains. The anti-CMG2 antibody
88 significantly reduced bFGF-induced corneal neovascularization in a concentration dependent

89 manner (Fig. 1B). In contrast, treatment with the anti-TEM8 antibody L2 at, a dose and schedule
90 previously shown to inhibit tumor growth in mice (20 mg/kg/week) [22] resulted in no significant
91 decrease in corneal neovascularization when compared to the vehicle control (Fig. 1C).
92 Together, these results show that inhibiting the interaction of CMG2 with its physiological ligand
93 significantly inhibits corneal angiogenesis, while inhibition of TEM8-ligand interaction does not.

94 To confirm the importance of CMG2 rather than TEM8 as a mediator of angiogenesis in
95 the cornea, we next sought to identify phenotypic changes that result from CMG2 or TEM8
96 knockout. We performed the corneal micropocket assay, using either bFGF or VEGF to induce
97 vessel growth in CMG2 and TEM8 knockout mice. CMG2 knockout (CMG2-/-) mice exhibit a
98 striking reduction in both bFGF (Fig 1E) and VEGF-induced (Fig 1F) corneal vascularization
99 compared to WT mice, confirming the importance of CMG2 in corneal angiogenesis.
100 Interestingly, female mice were particularly susceptible to this effect (Fig S1A-B), exhibiting a
101 >85% reduction in their response to VEGF (Fig S1B). In contrast, TEM8 knockout (TEM8-/-)
102 mice exhibited no significant reduction when stimulated with VEGF (Fig 1H) and only modest
103 reductions in bFGF-induced neovascularization (15%; $p<0.05$), (Fig 1G, S1C-D). These data
104 confirm that CMG2 plays a quantitatively substantial role in corneal neovascularization.

105 It remained possible that both anthrax toxin receptors might still be responsible for
106 mediating the anti-angiogenic effect of PA^{SSSR}. To assess this possibility, we evaluated the
107 efficacy of PA^{SSSR} in reducing corneal vascularization in CMG2-/- or TEM8-/- mice. Importantly,
108 CMG2-/- mice did not show reduction in bFGF-induced corneal angiogenesis (Fig2A). In
109 contrast, PA^{SSSR} treatment significantly reduced corneal neovascularization in both wild-type
110 control animals and TEM8-/- mice (Fig 2B). We conclude that CMG2 blockade is responsible for
111 the anti-angiogenic effects of PA^{SSSR}.

112 To establish whether the effect of CMG2 knockout or blockade is endothelial cell
113 intrinsic, we performed tube formation assays in Matrigel, using HMVEC cells, which express

114 both CMG2 and TEM8. We note that due to culture limitations, CMG2 ablation in HMVEC using
115 CRISPR is not possible; however, knockdown using siRNA was successful toknockdown (KD)
116 CMG2 or TEM8 (Fig 2C) and compared the anti-angiogenic effects of PA^{SSSR} on cells
117 expressing only one of the two receptors. In TEM8 KD cells (which primarily express CMG2),
118 PA^{SSSR} administration resulted in a concentration-dependent reduction in the extent of tube
119 network formation (Fig 2D-E). In contrast, tube formation in CMG2 KD cells was not altered by
120 PA treatment (Fig 2D-E). Together with knockout data described above, these results
121 demonstrate that PA^{SSSR} retains its anti-angiogenic effect in both TEM8-/- mice and TEM8 KD
122 HMVECs but not in CMG2-/- mice or CMG2 KD cells. Hence, we conclude that PA^{SSSR} exerts its
123 anti-angiogenic effects via CMG2 on endothelial cells.

124 We next worked to determine the CMG2-mediated endothelial process that PA^{SSSR}
125 disrupts to decrease angiogenesis. During angiogenesis, endothelial tip cells receive migratory
126 signals and orient themselves to migrate up a chemotactic gradient, while the stalk cells follow
127 and proliferate to form new vessel(s)[23] Thus, CMG2 could regulate angiogenesis by impacting
128 cell proliferation and/or cell migration. We have previously demonstrated that PA^{SSSR} affects cell
129 migration, but not proliferation in HMVEC[1], a primary endothelial cell type. Consistent with this
130 result, knockdown of neither CMG2 nor TEM8 knockdown significantly reduce HMVEC
131 proliferation (Fig S2A-D). We also observe no reduction in cell proliferation in EA.hy926
132 endothelial cells (a fusion of human umbilical vein cells with lung carcinoma cells) treated with
133 PA^{SSSR} under conditions that selectively target CMG2 (Fig S3A). Together, these data suggest
134 that CMG2 inhibition affect angiogenesis by modulating endothelial cell migration, rather than
135 cell proliferation.

136 Our data support the idea that PA^{SSSR} exerts its anti-angiogenic effects by competing
137 with interaction(s) between the CMG2 von Willebrand Factor A (vWA)[24, 25] domain (including the
138 metal ion-dependent adhesion site (MIDAS)[5, 26] and endogenous ligand(s). However, the

139 specific ligands that regulate angiogenesis by binding CMG2 remain unidentified. ECM proteins
140 are likely candidates because of CMG2's homology with integrins[25], modest available data
141 showing CMG2 interaction with ECM proteins[2], and the observation that in individuals with
142 hyaline fibromatosis syndrome (HFS), CMG2 mutations in the VWA domain result in widespread
143 accumulation and of extracellular matrix (ECM) proteins[8]. To verify interaction of CMG2 with
144 ECM proteins, we used ELISA to measure CMG2 K_d for a series of different ECM proteins
145 (Table S1; Fig S3 A-D). Interestingly, each of the ECM proteins tested (Collagens I, VI, laminin
146 and fibronectin) interacted with CMG2 with near-indistinguishable near-micromolar K_d values
147 (Table S1). Similar K_d values for different ECM proteins in these assays did not reflect artefacts
148 in the binding assay, since both positive and negative control assays (CMG2 + PA^{SSSR} and
149 CMG2 + PA^{SSSR} in the presence of EDTA, respectively) mirrored previously published K_d
150 values[18] . Previously published data on CMG2–matrix interactions, which[8] have indicated that
151 CMG2 may bind preferentially to collagens IV[2] or VI[8], are not necessarily at odds with this result.
152 Differences in protein preparation, matrix adhesion to wells, and number of binding sites per
153 molecule are all factors which influence relative signal observed in blot- and ELISA-based
154 assays. However, the similar affinity of CMG2 for the matrix proteins tested indicates that
155 CMG2, like integrins, may play a significant role in cell adhesion and motility through direct
156 interactions with the extracellular matrix.

157 To provide evidence for the assertion that PA^{SSSR} inhibits interaction between ECM and
158 CMG2, we performed *ex vivo* cell adhesion assays with EA.hy926 cells on plates coated with
159 different ECMs (Collagens I, IV, and VI, Human Fibronectin, and Laminin-111). Treatment with
160 PA^{SSSR} at concentrations identical to the CMG2 K_d value (200pM) significantly reduced
161 EA.hy926 cell adhesion on plates coated with each ECM, but not on uncoated plates (Fig S4B).
162 We note that at this concentration CMG2, but not TEM8, is blocked by PA^{SSSR}. Together, these

163 data suggest that CMG2 plays a role in mediating cell adhesion to ECM proteins[25], and that
164 PA^{SSSR} binding to CMG2 inhibits that interaction.

165 In angiogenesis a major function of cell adhesion is to enable cell migration. We
166 hypothesize that CMG2 may play a role in enabling cell movement. In that case, PA^{SSSR} would
167 inhibit cell migration as well as adhesion. Indeed, we find that PA^{SSSR} significantly reduces cell
168 migration on multiple different ECM substrates (Fig S4C-D). Specifically, we used fetal bovine
169 serum as chemoattractant in a microfluidic perfusion device which contains a perfusion chamber
170 that allows formation of a small molecule and macromolecule concentration gradient (data not
171 shown). In this setup, we can observe migration of individual cells in real time. As expected,
172 PA^{SSSR} treatment resulted in decreased migration over nearly all ECM surfaces (Fig S4C-D),
173 even at the 200pM concentration expected to result in only 50% bound CMG2. Combining these
174 adhesion and migration data, we conclude that ECM proteins mediate endothelial cell adhesion
175 and migration through interaction with CMG2, and that PA^{SSSR} can disrupt this interaction (Fig
176 S4B-D).

177 Notably, the nature of this migration assay allows us to compare two different aspects of
178 migration: initiation of cell movement (chemokinesis) and directional motion towards growth
179 factor-containing serum (chemotaxis). Surprisingly, targeting CMG2 in EA.hy926 cells with
180 PA^{SSSR} at the CMG2 Kd (200pM) showed a 70% decrease in observed chemotaxis on non-
181 coated surface (70%, $P<0.01$; Fig S4C. Given that we expect only 50% CMG2 occupancy at
182 these PA^{SSSR} concentrations, this chemotactic inhibition is dramatic. In contrast, the total
183 distance traveled by PA^{SSSR} treated cells was only modestly (~20%) reduced, compared to
184 untreated cells (Fig S4D). Thus, CMG2 targeting has a dramatic effect on chemotaxis but little
185 effect on chemokinesis.

186 Futher support for involvement of CMG2 in chemotaxis rather than chemokinesis is
187 provided by transwell migration experiments performed on CMG2 knockdown HMVEC cells.

188 Like many other traditional migration assays, the transwell assay does not provide a stable
189 chemoattractant gradient to allow chemotaxis measurement[27], and thus only measures
190 chemokinesis. Evaluation of these CMG2 knockdown cells via transwell migration assays
191 showed no significant difference between wild-type and CMG2 or TEM8 knockdown HMVEC
192 (Fig S4E), consistent with our previous observation that CMG2 inhibition impacts chemotaxis
193 but not chemokinesis.

194 We next examined the effect of CMG2 depletion on chemotactic migration in EA.hy926
195 cells, using CRISPR to target Exon1. Loss of CMG2 function in knockout cells was validated
196 with a flow cytometry assay in which uptake of a fluorescent PA-AF568 conjugate was
197 evaluated at CMG2 K_d 200pM (Fig 3A). CMG2 knockout cells showed substantial inhibition of
198 intracellular fluorescence relative to WT cells, and knockout cell fluorescence was
199 indistinguishable from that of negative control WT cells (Fig 3A). The ability of transfected
200 CMG2-mClover to rescue the PA uptake defect was confirmed, demonstrating that off-target
201 effects cannot explain loss of PA uptake in these cells (Fig 3A). Importantly, evaluation of the
202 migration of these EA.hy926 knockout cells in our microfluidic device demonstrated that while
203 WT cells migrated toward serum (Fig 3B), CMG2-/- cells migrated only in a random manner (Fig
204 3C). Significantly, knockout cells showed complete abolition of chemotactic migration (Fig 3E)
205 but only slight alteration of chemokinetic migration ($P<0.001$) (Fig 3F). To confirm that the loss
206 of chemotaxis was not a consequence of off target CRISPR effects, we complemented the
207 CMG2 mutation with a CMG2-clover expression vector and found that CMG2 add-back restored
208 EA.hy926 cell chemotaxis (Fig 3D-E). Hence, CMG2 is a critical component of chemotactic
209 sensing or response in these cells, and may play a role in regulating endothelial cell chemotaxis
210 *in vivo*. Of interest, CMG2 is required for reorientation of the mitotic spindle in zebrafish
211 embryos[28] suggesting that it might also play a role in orienting the microtubule cytoskeleton in a
212 chemotactic context.

213 We next investigated the effect of CMG2 deletion on developmental angiogenesis. To do
214 so, we compared retinal vessel development between WT and CMG2-/- mouse. We found that
215 the total vascular area was similar between the two genotypes (Fig. 4). However the vascular
216 growth pattern observed was different between knockout and WT mice, with knockout mice
217 having a more bush-like pattern versus the tree-like pattern observed in WT animals (Fig. 4A).
218 Careful quantitation showed that the total number of veins in the retina of WT and CMG2-/- mice
219 is similar (Fig 4A-B), but CMG2-/- mice have slightly fewer primary arteries (Fig 4A, C).
220 Importantly, CMG2-/- mice showed 2.5-fold more primary branches per artery than the WT cells
221 (Fig 4A, D). This difference in vessel patterning could be consistent with the loss of chemotactic
222 migration observed in knockout cells. We speculate that in the absence of CMG2, endothelial
223 cells effectively lose chemotactic signals (though haptotactic and other signals may be
224 retained), reducing effective directional movement. This hypothesized weaker response in
225 CMG2-/- mice to the developmental angiogenic gradient could leave some areas of the retina
226 with poor perfusion. Angiogenic signals from these areas could then lead to additional branching
227 to alleviate hypoxia, resulting in a vasculature that remains functional, but is patterned
228 differently.

229 CMG2 mediates chemotaxis that is induced by multiple different growth factors,
230 indicating that the process it regulates is core to that process. We have shown here that CMG2-
231 deficient mice showed potent reduction in corneal neovascularization induced by both bFG and
232 VEGF. In addition, Vink *et al*. has reported that CMG2 mediates migration of smooth muscle
233 cells towards PDGF[29]. Consistent with this observation, Reeves *et al*. have suggested that
234 CMG2 works closely with MT1-MMP, an important cofactor in PDGF signaling pathway[30].
235 Therefore, we have decided to measure endothelial cell migration under a gradient of individual
236 growth factor. Interestingly, EA.hy926 cells display a chemotactic migration towards bFGF and
237 PDGF, and can be significantly inhibited with 200pM of PA^{SSSR} treatment (Fig S5A). While cells

238 in insulin treatment didn't show much chemotactic migration (Fig S5A). We also measure
239 migration under the gradient of boiled FBS (Growth factors are denatured by boiling and
240 removed by centrifugation). Result show that EA.hy926 cells remain a high chemotaxis
241 phenotype, but it is not affected by PA treatment (Fig S5C). Neither the chemokinesis in all
242 these conditions were not affected by PA^{SSSR}, further suggest that CMG2 plays a critical role in
243 mediating chemotaxis towards some molecules that can be denatured at high temperature, like
244 bFGF, VEGF, and PDGF. Together, these data suggest that CMG2 may act as a central
245 regulator for chemotaxis that is initiated by a series of different growth factors. The mechanism
246 of CMG2's impact on chemotaxis will be important for developing new efficacious therapies to
247 treat pathological angiogenesis. It remains to be seen whether interaction of CMG2 with growth
248 factors receptors at the cell surface can be detected.

249

250

251 **Methods**:

252 Protein preparation

253 Cell culture

254 EA.hy926 (CRL-2922) cells are the result of a fusion of human umbilical vein
255 cells with lung carcinoma cells. Cells were cultured in 10% FBS + DMEM and incubated
256 at 37°C in a humidified environment with 5% CO_2 until ready for passaging.

257

258 EA.hy cell proliferation assay

259 15,000 EA.hy926 cells were seeded into each well in a 96 well plate and incubated for 1
260 h to attach. After cell attachment, media with treatments were added. Ethanol fixed cells were
261 used as negative control. After a 24 h incubation, 20 µL CellTiter-Blue Reagent (Promega) was
262 added to each well for 4 h. Fluorescence signal (Ex: 560nm / Em: 590nm) was measured using
263 a BioTek Synergy H2 plate reader. All readings were normalized to the non-treated control.

264

265 Cell ASIC migration assay

266 The assay protocol followed the CellASIC ONIX M04G-02 Microfluidic Gradient Plate
267 User Guide. All media put into the plate (excepting the cell suspension) was filtered through a
268 0.2 µm syringe filter. EA.hy cells (3 x 10^6 cells/mL) were loaded in and incubated overnight with
269 DMEM + 10% FBS under flow at 37°C. Assays were then performed with a stable gradient of
270 DMEM + 0 – 10% FBS with or without peptide treatment. Brightfield images at 10x magnification
271 were taken every 10 min over 12 h on an Olympus IX73 microscope and the ORCA-Flash4.0
272 camera (Hamamatsu). Individual cells were tracked with Image J manual tracking plugin. Data
273 was transferred into the ibidi Chemotaxis and Migration Tools 2.0. to export endpoint y

displacement and accumulated displacement. P-values were calculated using Student's *t*-test and error bars are standard error of the mean (n=50).

CMG2 ECM ELISA

All steps were performed at room temperature unless otherwise indicated. For binding assays, matrix protein (Rockland Immunochemicals, Corning, EMD Millipore) was adsorbed onto 96-well polyethylene plates (Greiner) by incubating 2 ug/mL matrix protein in HBS with 2 mM Mg^{2+} and Ca^{2+} (Buffer A) in individual wells at 4° C overnight. Bacillus anthracis protective antigen (PA) was treated similarly but was incubated at 1 μM in the same buffer. After incubation, wells were washed 3x with Buffer A and blocked with 5% BSA (GoldBio) in HBS with 2 mM Mg^{2+}, 2 mM Ca^{2+}, and 0.1% Tween-20 (Buffer B) for 1 hour. Blocking was followed by 3 washes with Buffer B, after which varying concentrations of a biotinylated CMG2-AviTag construct (for matrix, 2138 to 10 μM; for PA, 4 μM to 1 pM) were dissolved in Buffer B and incubated in wells for 4 hours. After incubation with CMG2-AviTag, wells were again washed 3 times, after which streptavidin-HRP (Thermo Scientific) diluted in Buffer B with 5% BSA was incubated in wells for 1 hour. Wells were then washed 6 times with Buffer B, after which 1x TMB solution (Thermo Scientific) was added to wells. Once color was visible in wells, reaction was quenched with 0.2 M H_2SO_4. Wells were read out in a BioTek H4 Hybrid plate reader (BioTek) by quantifying well absorbance at 450 nm. Data were analyzed in Microsoft Excel, and Kd values were calculated in MATLAB using the sigm_fit function.

Adhesion assay

EA.hy 926 cells were grown in DMEM supplemented with 10% FBS. 20μg/mL collagen I, IV, VI, laminin, fibronectin, PA^{SSSR}, and BSA were preared in PBS and coated in 96well plate (100□g/well) overnight at 4ºC. After coating, collagen I, IV, VI, laminin, fibronectin, PA^{SSSR}, and BSA were removed and 5% BSA were coated for 1 hour. Cells were deprived with serum by

298 scraped and cells were at 100g for 10 minutes and the supernatant was discarded. Cells then
299 resuspended at 2-3x10^5 cells/mL in DMEM. 100μL of cells were added to each of the coated
300 wells. The plate was incubated at 37°C for 1 hour to allow the cells to adhere on the surface.
301 Each well was washed gently for two times using warm serum-free DMEM by multi-channel
302 pipettor. 100μL of serum free DMEM and 20μL of cell-titler blue (Promega Cat#G8080) were
303 added into each well, and incubated for 4 hours at 37°C. After 4 hours incubation, fluorescent
304 signal of 96 well plate was measured at $560_{Ex}/590_{Em}$ by a plate reader.

305 EAhy 926 CMG2 KO development:

306 HEK 293T cells (3.8 x 10^6 cells) were seeded in 10cm tissue culture dish for 18 hours.
307 12μg of pCMV, 5μg of pVSVG, 12.5μg of Lenti-CRISPR (targeting CMG2 exon 1, sgRNA
308 sequence: GCACCAACAGCCACAGCCCG), 90μL of 1mg/mL PEI and 600μL of serum-free
309 DMEM were mixed into a tube and incubated for 15 minutes before adding to the 10cm culture
310 dish. The dish was replaced with 10mL of 10% FBS DMEM in 4 hours and followed by 48 hours
311 incubation. Media was removed from the transfected cells into a conical tube, and was spin at
312 2500g for 3 minutes to remove debris. The supernatant (lentivirus) and 10μg/mL polybrene were
313 added to 40% confluent EA.hy926 cells and incubated for 24 hours. The next day, media was
314 removed, fresh 10% FBS DMEM and 1μg/mL puromycin were added to the plate for 3-5 days.
315 After 3-5 days, the cells that survived in the selection were diluted into single colony in 96 well
316 plate.

317 PA uptake flow cytometry:

318 CMG2 KO EA.hy 926 cells and WT EA.hy926 cells were split in 12 well plate at 50%
319 confluent. 200pM PA-Alexa Fluor 546 was added into each well and incubated overnight. Then
320 cells were trypsinized and resuspended into a microcentrifuge tube. Cells were washed once

321 with complete media. Then 50,000 cells of each condition were sent to Cytoflex (RIC facility at
322 BYU). Data was collected and analyzed in our lab by using FlowJo software.

323

324 Corneal micropocket assay

325 The corneal micropocket assay was performed as described[16] using pellets containing 80 ng
326 of basic fibroblast growth factor (bFGF) or 180 ng of human carrier-free recombinant vascular
327 endothelial growth factor (VEGF; R&D Systems) in C57BL/6J mice. The treated groups received
328 daily or twice daily i.p injections for 5 (bFGF) or 6 (VEGF) consecutive days of protein in PBS.
329 Treatment was started on the day of pellet implantation; control mice received only vehicle i.p. The
330 area of vascular response was assessed on the 5th (bFGF) or 6th (VEGF) postoperative day using a
331 slit lamp. Typically, at least 10 eyes per group were measured.

332 HMVEC proliferation assay

333 Human microvascular endothelial cells (Cambrex) were maintained in EGM-2 (Cambrex)
334 according to the vendor's instructions and used before passage 7. On day 0, proliferating cultures of
335 BCE or HMVEC-d cells were seeded at ~10% confluence into 96-well plates. After attachment,
336 medium was exchanged for medium containing 1 pmol/L to 1 μmol/L of the indicated protein. Cells
337 were allowed to grow for 7 days and then quantified using CyQUANT (Invitrogen) according to
338 manufacturer's directions. The degree of proliferation in culture was measured by comparing wells in
339 each plate fixed in absolute ethanol on day 0 with experimental wells, with fold proliferation
340 calculated by dividing CyQUANT fluorescence in experimental wells by that in day 0 wells. Groups
341 were compared using Student's *t* test, with Bonferroni correction where appropriate.

342 HMVEC Trans-well migration assay

343 Human microvascular endothelial cells were maintained as above. Polycarbonate Transwell
344 inserts, 6.5 mm diameter with 8.0 μm pores, were coated with fibronectin (BD Biosciences). Cells

345 were harvested and resuspended in EBM (Cambrex) containing 0.1% bovine serum albumin (Fisher
346 Chemical). Cells (10,000 per well) were plated onto wells containing medium alone or medium
347 containing the molecule to be tested. These wells were suspended above wells containing 5 to 10
348 ng/mL recombinant human VEGF (R&D Systems) or full serum medium. Cells were allowed to
349 migrate for 4 h. Membranes were rinsed once in PBS and then fixed and processed using Diff-Quick
350 (Dade Diagnostics). Cells on the top of the membrane were removed using cotton-tipped
351 applicators, and the membrane was removed from the insert using a scalpel. Membranes were then
352 mounted on slides, and the number of cells in a microscopic field was counted manually.

353 HMVEC CMG2 / TEM8 KD

354

355 HMVEC tube formation assay

356 Human microvascular endothelial cells were maintained as above. Before the assay, a 1- to
357 2-mm layer of Matrigel was plated into the wells of a 12-well cluster. Approximately 10^5 cells were
358 plated on this layer in EGM-2. Plates were examined at 12, 14, 16, 18, and 24 h for differences in
359 network formation. In each experiment, good network formation was observed in untreated control
360 wells.

361 CMG2 and TEM8 KO mice

362

363 Western Blotting

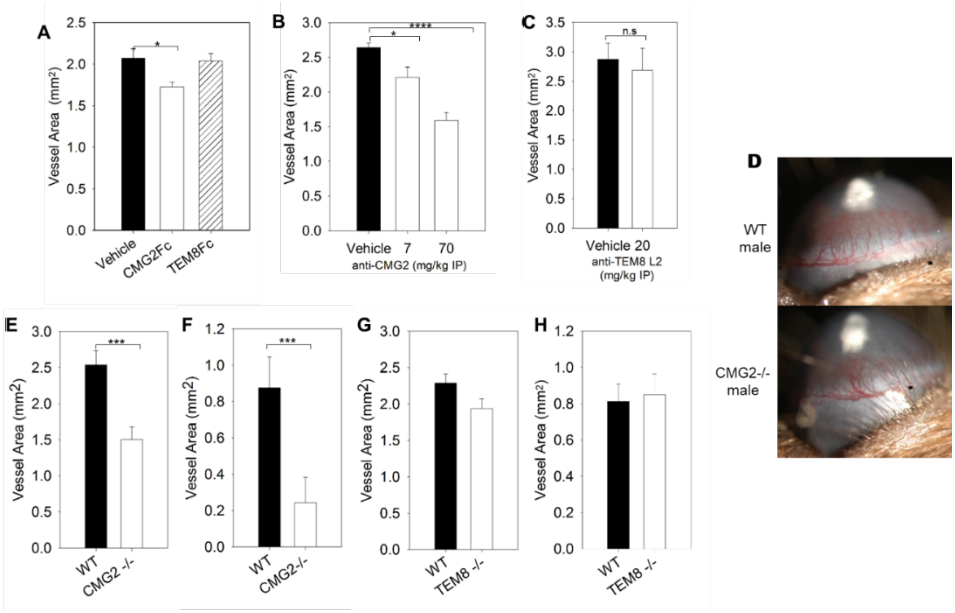

Figure 1. Blocking the interactions of CMG2 with its natural ligand inhibits both FGF and VEGF induced corneal neovascularization *in vivo.* (A) Corneal micropocket assay on mice treated with soluble ECD of either CMG2 or TEM8, via intraperitoneal injection. (B-C) Corneal micro-pocket assay on mice treated with either anti-CMG2 antibody (B) or anti-TEM8 L2 anti-body (C). Corneal neovascularization in these assays was induced by bFGF before treatment; vessel area on both the left and right corneas were measured from each mouse. (D) Representative image of corneal neovascularization in both wild type (WT) and CMG2 -/- male mice. (E-F) Comparison of corneal neovascularization between WT and CMG2-/- mice induced by either bFGF (E) or VEGF (F). CMG2-/- mice showed significant reductions in neovascularization for both bFGF- and VEGF-induced angiogenesis. (G-H) A similar experiment was performed with WT and TEM8-/- mice with either bFGF (G) or VEGF (H). Data presented are pooled from both genders. Error bars are standard error of mean, * $p<0.05$; ** $p<0.01$; *** $p<0.001$.

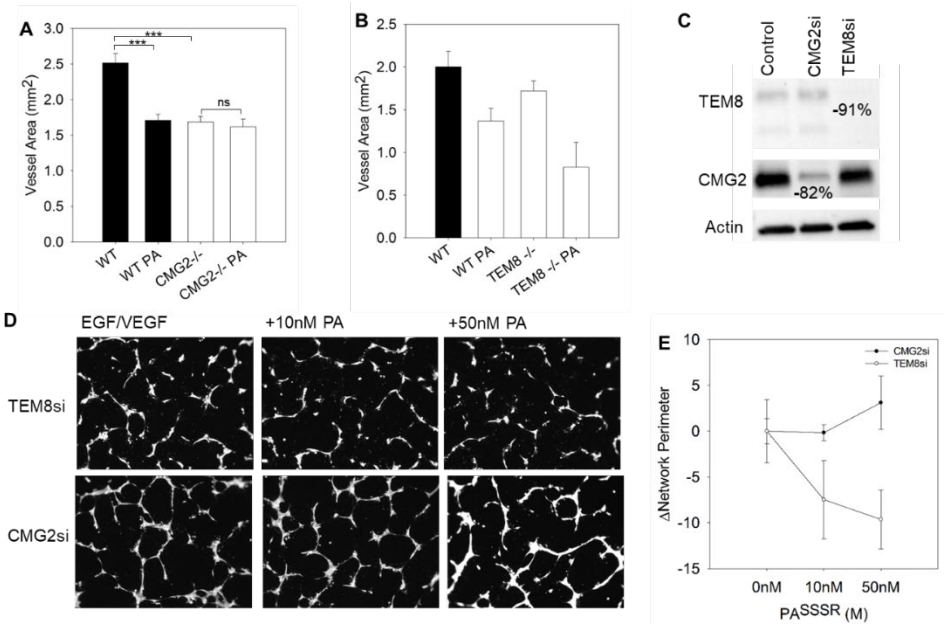

Figure 2. CMG2 is the main mediating receptor of PA^{SSSR}-induced angiogenic inhibition. (A) Comparative levels of bFGF-induced corneal neovascularization between CMG2-/- and WT mice treated with or without PA^{SSSR}, and (B) TEM8-/- and WT mice treated with or without PA^{SSSR}. Results showed that PA^{SSSR} reduced vessel formation on TEM8-/- mice but not CMG2-/- mice. . Error bars are standard error of mean. (C) Western blot of HMVEC lysates with either CMG2 knockdown (CMG2si) or TEM8 knockdown (TEM8si). Band intensity was normalized to control (untreated cells). (D) EGF- and VEGF-induced tubule formation assays with both CMG2si- and TEM8si-HMVEC, treated with or without different concentrations of PA^{SSSR}. (E) Quantification of tube formation assays by counting the number of networks on each field. Error bars are standard deviation.

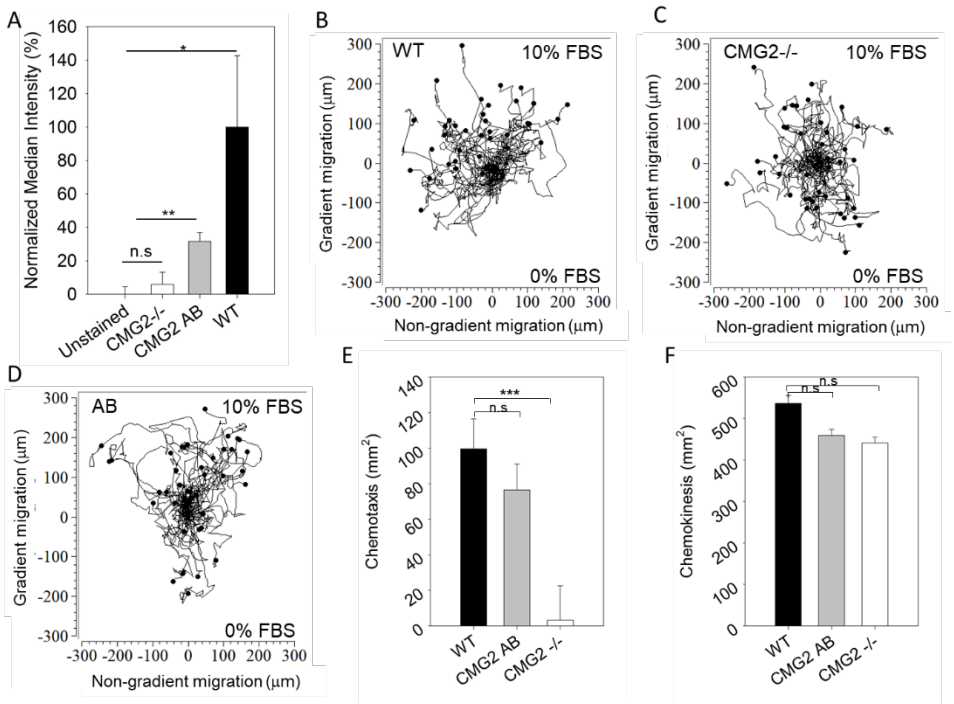

Figure 3. CMG2 KO endothelial cells lose the ability to migrate toward chemoattractants . (A) Differential PA-AF586 conjugate uptake by wild type (WT), CMG2 add back (AB) CMG2 knockout (CMG2 -/-) EA.hy926 cells via flow cytometry (10,000 cells per condition). Median fluorescence intensiy of each condition was normalized against WT signal after subtracting from the unstain control. Error bars are normalized standard deviation from three individual replicates.. (B) Aggregated track plots of individual EA.hy926 cell migration in the CellASIC migration chamber. Both WT cells (B), CMG2-/- cells (C), and CMG2 AB cells were subjected to an FBS gradient. (E-F) Quantification of both Ea.hy926 chemotaxis (displacement toward gradient, E) and Chemokenesis (total migration, F) in the CellASIC migration assay. * $p<0.05$; ** $p<0.01$; *** $p<0.001$; n.s not significant

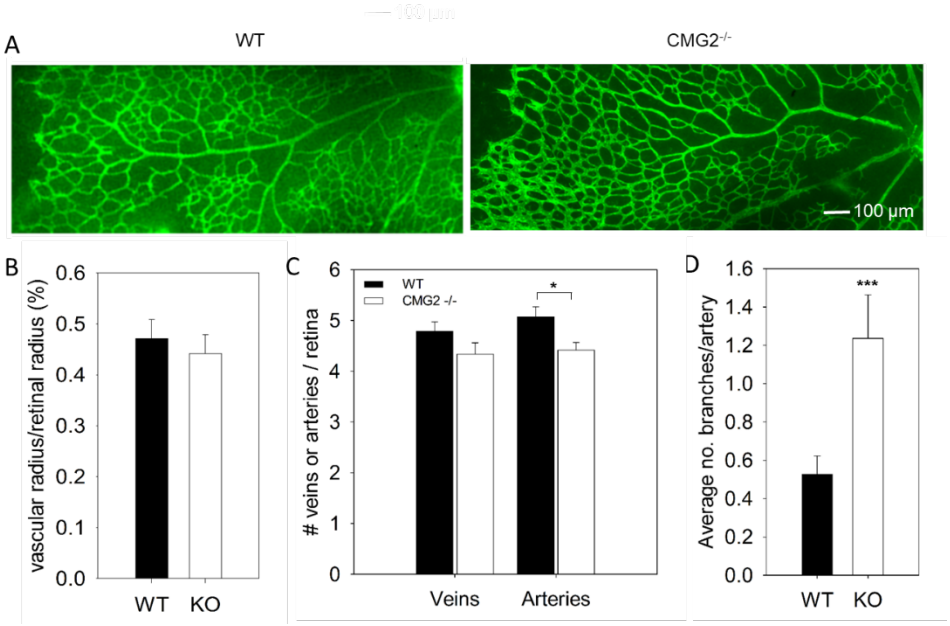

Figure 4. CMG2 KO increases vessel branching in the mouse retina. (A) Representative mages of vessel formation in the retina of both WT (left) and CMG2-/- (right) mice. (B-D) Quantified vessel formation from retinal assays. (B) Comparison of vascular radius, normalized to the retinal radius, between WT and CMG2-/- mice. (C) Quantification of arterial branching in both WT and CMG2-/- mouse retinas. (D) Artery and vein counts per retina as in WT and CMG2-/- mice. CMG2-/- mouse retinas exhibit fewer veins and arteries than WT, but only artery count is significantly lower than WT mice.

419 Supplementary Figure 1

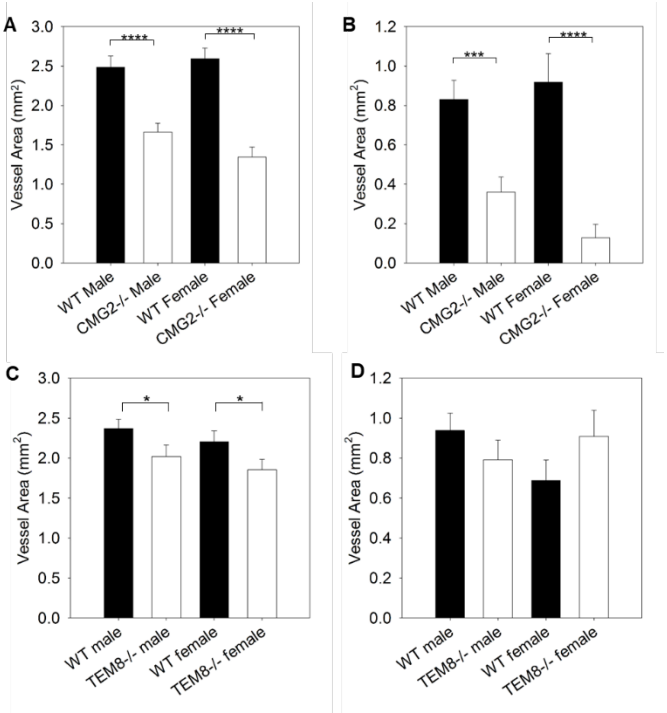

420 **Supplementary Figure S1. Gender-specific quantification of bFGF- and VEGF-induced**
421 **corneal vascularization in WT, CMG2 KO, and TEM8 KO mice.** (A-B) Quantification of (A)
422 bFGF-induced and (B) VEGF-induced neovascularization in male and female CMG2-/- mice as
423 compared to WT. (C-D) Quantification of (C) bFGF-induced and (D) VEGF-induced
424 neovascularization in male and female TEM8-/- mice as compared to WT. For both genders,
425 greater decreases in corneal vascularization were observed in CMG2 KO than for TEM8 KO.

426

427

428 Supplementary Figure 2

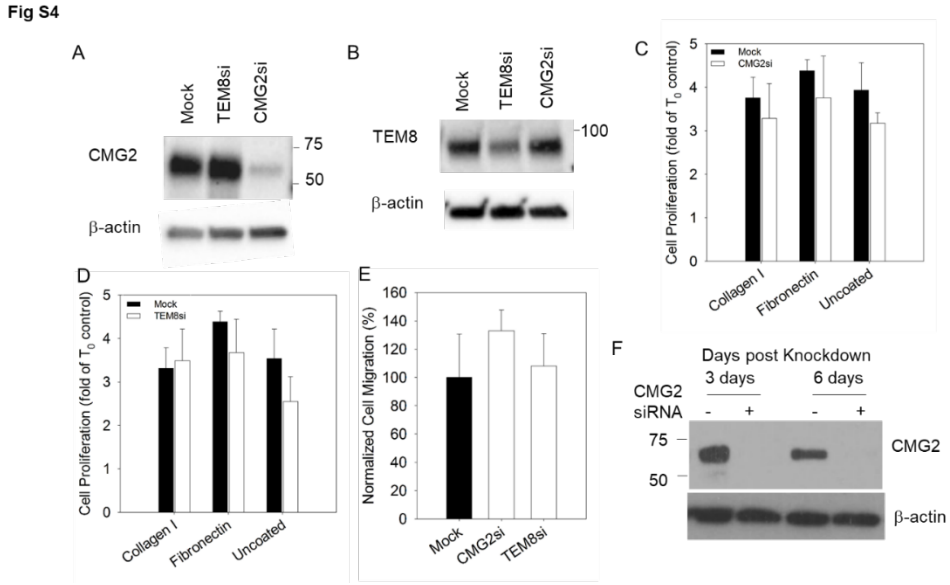

429

430

431 **Supplementary Figure S2. Effects of CMG2 and TEM8 siRNA-mediated knockdown on**
432 **Ea.hy926 cell proliferation and migration.** (A-B) Western blot analysis of Ea.hy926 lysates for
433 (A) CMG2 and (B) TEM8 before and after introduction of siRNA. (C-D) Proliferation of both WT
434 and siRNA-treated Ea.hy926 cells with both (C) CMG2-specific and (D) TEM8-specific siRNA.
435 Proliferation was not significantly altered from WT in either CMG2-targeted or TEM8-targeted
436 cells. (E) Migration of WT, CMG2 siRNA and TEM8 siRNA-treated Ea.hy926 cells. No
437 significant difference in migration was observed from WT. (F) Western blot analysis of Ea.hy926
438 lysates for CMG2 expression 3 days and 6 days after addition of siRNA.

439

440 Table S1

Protein	kD (nM)	Std. Dev	Repeats
Collagen I	500	141	3
Collagen VI	800	411	3
Laminin-111	500	158	2
Fibronectin	500	141	3
PA (positive control)	0.46	0.047	3
PA w/EDTA (neg. control)	None	N/A	2

441

442 **Supplementary Table S1. CMG2 binds several broadly expressed matrix proteins with**
443 **high affinity.** Results of an ELISA-based quantification of CMG2 binding to several broadly-
444 expressed matrix proteins, including collagens, laminin-111, and fibronectin. For positive
445 control, PA was assayed for binding to CMG2. Such similar affinities between matrix proteins
446 indicate that CMG2 shows no preference for binding to any one of the matrix proteins assayed.

447

448 Supplementary Figure S3

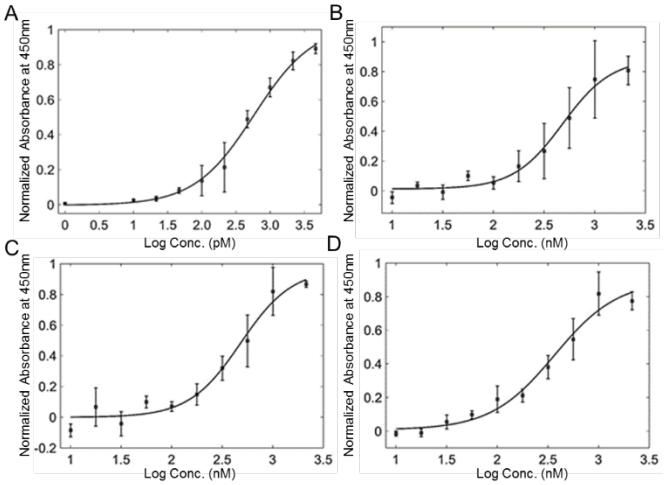

449

450 **Supplementary Figure** S3. Binding of CMG2 to extracellular matrix proteins, as determined by
451 ELISA. Proteins were coated on wells, after which CMG2-GST-biotin was added and signal
452 read out with streptavidin-HRP/TMB. KD values were calculated by fitting each dataset to a 4-
453 parameter logistic curve. A, positive control (PA); B, fibronectin; C, collagen I; D, collagen VI. PA
454 x axis scale is logarithmic with pM concentration units; all others are logarithmic with nM
455 concentration values. Y axis is normalized absorbance at 450 nm. Collagen IV and laminin-111
456 were also assayed for binding, but curves are not displayed due to poor fit. In each case, similar
457 binding affinites (500 nM-1 uM) were observed (see Supplementary Table S1).

458 Supplementary Figure 4

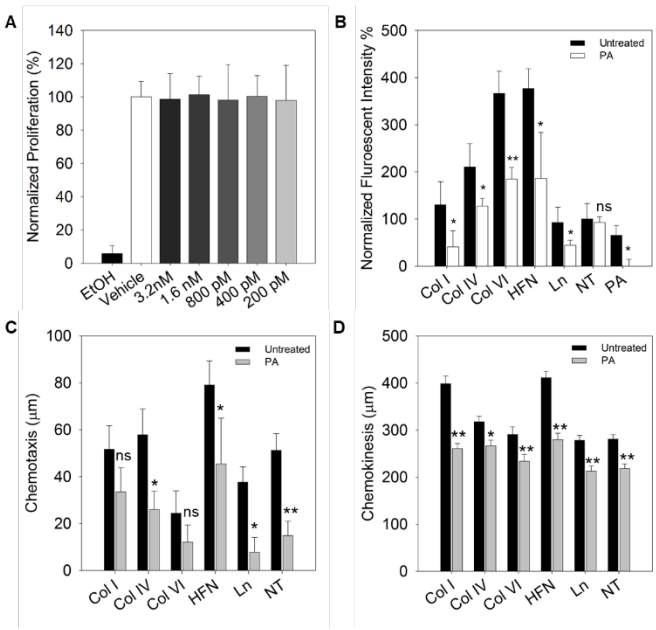

459

460 **Supplementary Figure S4. Matrix binding to CMG2 is an important component of cell**
461 **adhesion and migration.** (A) EA.hy926 endothelial cell proliferation in different concentrations
462 of PA^{SSSR}. Ethanol (EtOH) treated cells was used as the negative control. (B) EA.hy926
463 endothelial cell adhesion to plates coated with various matrix proteins, or no ECM proteins
464 ("NT"), both with and without 200 pM PA. Addition of PA significantly inhibits adhesion to
465 matrix-coated plates. Adhesion to uncoated plates was not affected by PA^{SSSR} treatment. (C-D)
466 EA.hy926 migration on different ECM coated surface and compare to the PA^{SSSR} treatment.
467 Chemotaxis are the vertical displacement measured towards a serum gradient form across the
468 migration chamber (C). While chemokinesis are measured by total distance cell migrated in
469 random direction (D). statistic significance between untreated and PA treated cell was
470 calculated by student T.Test. Error bars are standard deviation of mean, * $p<0.05$; ** $p<0.01$; n.s
471 not significant

472

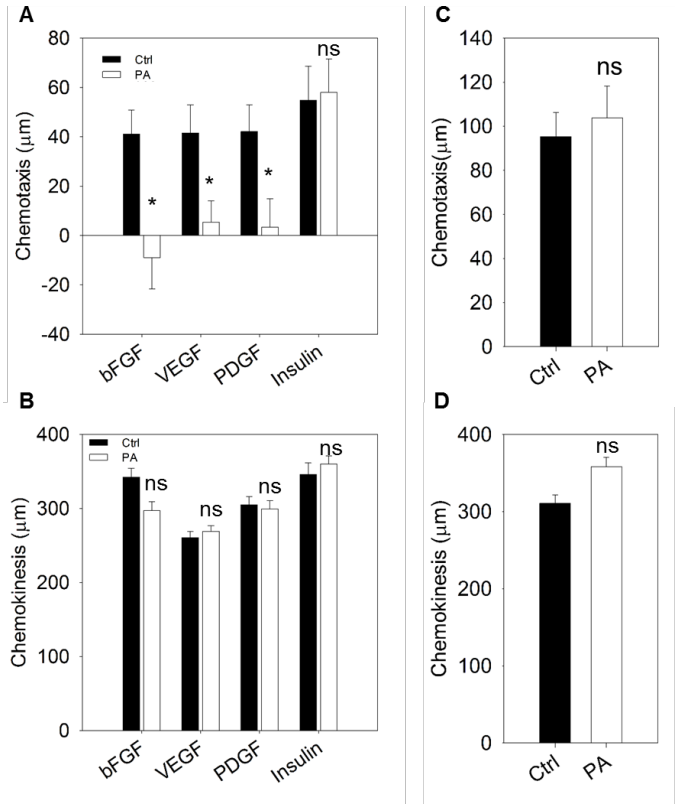

Supplementary Figure S5. CMG2 directs cell chemotaxis towards various growth factors in serum. (A-B) EA.hy926 endothelial cell migration under a gradient of various growth factors (20ng/mL bFGF and PDGF, 300ng/mL VEGF) and fetal bovine serum (FBS; 10%). Displacement on Y direction (direction towards chemoattractant gradient) was measured and displayed as chemotaxis (A). Total migration distance was measured and displayed as chemokinesis (B). (C-D) EA.hy926 endothelial cell migration under a gradient of boiled FBS (10%). FBS was boiled and centrifuged to remove denatured and precipitated proteins. Supernatant (10%) was used in the migration to measure chemotaxis (C) and chemokinesis (D). 200pM of PA^{SSSR} was used to treat the cells in each condition and compared with non-treated cells (Ctrl). 40 cells were tracked from each conditions and error bar is standard deviation of three individual replicates. * $p<0.05$; ** $p<0.01$; n.s not significant

References:

[1] Rogers, M. S., Christensen, K. A., Birsner, A. E., Short, S. M., Wigelsworth, D. J., Collier, R. J., and D'Amato, R. J. (2007) Mutant anthrax toxin B moiety (protective antigen) inhibits angiogenesis and tumor growth, *Cancer Res 67*, 9980-9985.

[2] Bell, S. E., Mavila, A., Salazar, R., Bayless, K. J., Kanagala, S., Maxwell, S. A., and Davis, G. E. (2001) Differential gene expression during capillary morphogenesis in 3D collagen matrices: regulated expression of genes involved in basement membrane matrix assembly, cell cycle progression, cellular differentiation and G-protein signaling, *J Cell Sci 114*, 2755-2773.

[3] Cryan, L. M., Bazinet, L., Habeshian, K. A., Cao, S., Clardy, J., Christensen, K. A., and Rogers, M. S. (2013) 1,2,3,4,6-Penta-O-galloyl-beta-D-glucopyranose inhibits angiogenesis via inhibition of capillary morphogenesis gene 2, *J Med Chem 56*, 1940-1945.

[4] E, G. D., Carrero, P., Madrona, A., Rodriguez-Salamanca, P., Martinez-Gualda, B., Camarasa, M. J., Jimeno, M. L., Bennallack, P. R., Finnell, J. G., Tsang, T. M., Christensen, K. A., San-Felix, A., and Rogers, M. S. (2019) Galloyl Carbohydrates with Antiangiogenic Activity Mediated by Capillary Morphogenesis Gene 2 (CMG2) Protein Binding, *J Med Chem 62*, 3958-3970.

[5] Scobie, H. M., Rainey, G. J. A., Bradley, K. A., and Young, J. A. T. (2003) Human capillary morphogenesis protein 2 functions as an anthrax toxin receptor, *P Natl Acad Sci USA 100*, 5170-5174.

[6] Lacy, D. B., Wigelsworth, D. J., Scobie, H. M., Young, J. A., and Collier, R. J. (2004) Crystal structure of the von Willebrand factor A domain of human capillary morphogenesis protein 2: an anthrax toxin receptor, *Proc Natl Acad Sci U S A 101*, 6367-6372.

[7] van der Goot, G., and Young, J. A. (2009) Receptors of anthrax toxin and cell entry, *Mol Aspects Med 30*, 406-412.

[8] Burgi, J., Kunz, B., Abrami, L., Deuquet, J., Piersigilli, A., Scholl-Burgi, S., Lausch, E., Unger, S., Superti-Furga, A., Bonaldo, P., and van der Goot, F. G. (2017) CMG2/ANTXR2 regulates extracellular collagen VI which accumulates in hyaline fibromatosis syndrome, *Nat Commun 8*, 15861.

[9] Bayram, Y., Pehlivan, D., Karaca, E., Gambin, T., Jhangiani, S. N., Erdin, S., Gonzaga-Jauregui, C., Wiszniewski, W., Muzny, D., Elcioglu, N. H., Yildirim, M. S., Bozkurt, B., Zamani, A. G., Boerwinkle, E., Gibbs, R. A., Lupski, J. R., and Geno, B. H. C. M. (2014) Whole Exome Sequencing Identifies Three Novel Mutations in ANTXR1 in Families with GAPO Syndrome, *American Journal of Medical Genetics Part A 164*, 2328-2334.

[10] Stranecky, V., Hoischen, A., Hartmannova, H., Zaki, M. S., Chaudhary, A., Zudaire, E., Noskova, L., Baresova, V., Pristoupilova, A., Hodanova, K., Sovova, J., Hulkova, H., Piherova, L., Hehir-Kwa, J. Y., de Silva, D., Senanayake, M. P., Farrag, S., Zeman, J., Martasek, P., Baxova, A., Afifi, H. H., St Croix, B., Brunner, H. G., Temtamy, S., and Kmoch, S. (2013) Mutations in ANTXR1 cause GAPO syndrome, *Am J Hum Genet 92*, 792-799.

[11] Landing, B. H., and Nadorra, R. (1986) Infantile systemic hyalinosis: report of four cases of a disease, fatal in infancy, apparently different from juvenile systemic hyalinosis, *Pediatr Pathol 6*, 55-79.

[12] Tanaka, K., Ebihara, T., Kusubata, M., Adachi, E., Arai, M., Kawaguchi, N., Utsunomiya, J., Miki, Y., Hiramoto, M., Hattori, S., and Irie, S. (2009) Abnormal collagen deposition in fibromas from patient with juvenile hyaline fibromatosis, *J Dermatol Sci 55*, 197-200.

[13] Deuquet, J., Lausch, E., Superti-Furga, A., and van der Goot, F. G. (2012) The dark sides of capillary morphogenesis gene 2, *Embo J 31*, 3-13.

[14] Glover, M. T., Lake, B. D., and Atherton, D. J. (1991) Infantile systemic hyalinosis: newly recognized disorder of collagen?, *Pediatrics 87*, 228-234.

531 [15] Cryan, L. M., and Rogers, M. S. (2011) Targeting the anthrax receptors, TEM-8 and CMG-2, for anti-
532 angiogenic therapy, *Front Biosci (Landmark Ed) 16*, 1574-1588.
533 [16] Rogers, M. S., Birsner, A. E., and D'Amato, R. J. (2007) The mouse cornea micropocket angiogenesis
534 assay, *Nat Protoc 2*, 2545-2550.
535 [17] Bradley, K. A., Mogridge, J., Mourez, M., Collier, R. J., and Young, J. A. T. (2001) Identification of the
536 cellular receptor for anthrax toxin, *Nature 414*, 225-229.
537 [18] Wigelsworth, D. J., Krantz, B. A., Christensen, K. A., Lacy, D. B., Juris, S. J., and Collier, R. J. (2004)
538 Binding stoichiometry and kinetics of the interaction of a human anthrax toxin receptor, CMG2,
539 with protective antigen, *J Biol Chem 279*, 23349-23356.
540 [19] Martchenko, M., Jeong, S. Y., and Cohen, S. N. (2010) Heterodimeric integrin complexes containing
541 beta1-integrin promote internalization and lethality of anthrax toxin, *Proc Natl Acad Sci U S A*
542 *107*, 15583-15588.
543 [20] Scobie, H. M., Thomas, D., Marlett, J. M., Destito, G., Wigelsworth, D. J., Collier, R. J., Young, J. A.,
544 and Manchester, M. (2005) A soluble receptor decoy protects rats against anthrax lethal toxin
545 challenge, *J Infect Dis 192*, 1047-1051.
546 [21] Scobie, H. M., Wigelsworth, D. J., Marlett, J. M., Thomas, D., Rainey, G. J., Lacy, D. B., Manchester,
547 M., Collier, R. J., and Young, J. A. (2006) Anthrax toxin receptor 2-dependent lethal toxin killing
548 in vivo, *PLoS Pathog 2*, e111.
549 [22] Chaudhary, A., Hilton, M. B., Seaman, S., Haines, D. C., Stevenson, S., Lemotte, P. K., Tschantz, W. R.,
550 Zhang, X. M., Saha, S., Fleming, T., and St Croix, B. (2012) TEM8/ANTXR1 Blockade Inhibits
551 Pathological Angiogenesis and Potentiates Tumoricidal Responses against Multiple Cancer
552 Types, *Cancer Cell 21*, 212-226.
553 [23] Gerhardt, H., Golding, M., Fruttiger, M., Ruhrberg, C., Lundkvist, A., Abramsson, A., Jeltsch, M.,
554 Mitchell, C., Alitalo, K., Shima, D., and Betsholtz, C. (2003) VEGF guides angiogenic sprouting
555 utilizing endothelial tip cell filopodia, *J Cell Biol 161*, 1163-1177.
556 [24] Lacy, D. B., Wigelsworth, D. J., Scobie, H. M., Young, J. A. T., and Collier, R. J. (2004) Crystal structure
557 of the von Willebrand factor A domain of human capillary morphogenesis protein 2: An anthrax
558 toxin receptor, *P Natl Acad Sci USA 101*, 6367-6372.
559 [25] Whittaker, C. A., and Hynes, R. O. (2002) Distribution and evolution of von Willebrand/integrin A
560 domains: widely dispersed domains with roles in cell adhesion and elsewhere, *Mol Biol Cell 13*,
561 3369-3387.
562 [26] Gao, M., and Schulten, K. (2006) Onset of anthrax toxin pore formation, *Biophys J 90*, 3267-3279.
563 [27] Hulkower, K. I., and Herber, R. L. (2011) Cell migration and invasion assays as tools for drug
564 discovery, *Pharmaceutics 3*, 107-124.
565 [28] Castanon, I., Abrami, L., Holtzer, L., Heisenberg, C. P., van der Goot, F. G., and Gonzalez-Gaitan, M.
566 (2013) Anthrax toxin receptor 2a controls mitotic spindle positioning, *Nat Cell Biol 15*, 28-39.
567 [29] Vink, J. Y., Charles-Horvath, P. C., Kitajewski, J. K., and Reeves, C. V. (2014) Anthrax toxin receptor 2
568 promotes human uterine smooth muscle cell viability, migration and contractility, *Am J Obstet*
569 *Gynecol 210*, 154 e151-158.
570 [30] Reeves, C. V., Wang, X., Charles-Horvath, P. C., Vink, J. Y., Borisenko, V. Y., Young, J. A., and
571 Kitajewski, J. K. (2012) Anthrax toxin receptor 2 functions in ECM homeostasis of the murine
572 reproductive tract and promotes MMP activity, *Plos One 7*, e34862.

573

574

575

576

577

578

579

580

581 Supplementary note:

582 1. bFGF was more used in corneal assays because we saw a better angiogenic effects

583 2. 200pM PA was targeting CMG2